International Journal of Environmental Protection and Policy
2023; 11(1): 10-20
http://www.sciencepublishinggroup.com/j/ijepp
doi: 10.11648/j.ijepp.20231101.12
ISSN: 2330-7528 (Print); ISSN: 2330-7536 (Online)

Land Use / Land Cover Change Detection and Its Driving Factors in *Suluh* River Basin, Northern Highland Part of Ethiopia

Hailay Hagos[1, 2, *], Amare Sewnet[1, 3], Emiru Birhane[4, 5]

[1]Department of Geography and Environmental Studies, Bahir Dar University, Bahir Dar, Ethiopia

[2]Department of Geography and Environmental Studies, Debre Tabor University, Debre Tabor, Ethiopia

[3]Spearheads Climate Resilient Green Economy Research in North Western Ethiopia (BDU-IUC Programme), Bahir Dar University, Bahir Dar, Ethiopia

[4]Department of Land Resources Management and Environmental Protection, Mekelle University, Mekelle, Ethiopia

[5]Faculty of Environmental Sciences and Natural Resource Management Norwegian, University of Life Sciences, Åas, Norway

Email address:

hailayhagos4@gmail.com (Hailay Hagos), Amare1974@gmail.com (Amare Sewnet), emiru.birhane@mu.edu.et (Emiru Birhane)

[*]Corresponding author

To cite this article:

Hailay Hagos, Amare Sewnet, Emiru Birhane. Land Use / Land Cover Change Detection and Its Driving Factors in *Suluh* River Basin, Northern Highland Part of Ethiopia. *International Journal of Environmental Protection and Policy*. Vol. 11, No. 1, 2023, pp. 10-20. doi: 10.11648/j.ijepp.20231101.12

Received: December 20, 2022; **Accepted**: February 9, 2023; **Published**: February 21, 2023

Abstract: The *Suluh* river basin is subjected to land use and land cover change due to population pressure, improper farming practices, lack of alternative non-farm activities, and rugged topography. Yet, land use/land cover change detection and its driving factors have not been applied in the study area. Thus, the current study detected land use and land use change and identified the drivers for it in the *Suluh* river basin, the northern highland part of Ethiopia. Landsat image data and Ancillary data sources were used to achieve the objectives. With the aid software's of *eCognition* Developer 9.2 and IDRISI *Selva* 17.3, images were classified and changes were detected. Both qualitative and quantitative data were analyzed. According to the study's findings, between 1990 and 2018, cultivated land expanded by 7.98%, plantation land by 43.7%, built up land by 135.5%, and bar land by 9.8%. A decline trend was found to exist for water bodies by 79.6%, pasture land by 48.6%, shrub and bush land by 61.7%, and forest land by 576.7%. Thus, in order to implement sustainable land management practices in the *Suluh* river basin, land use planners should take into account information about land use and land cover change, as well as the corresponding drivers.

Keywords: Change Detection, Drivers, Fuzzy Classification, Image Segmentation, Multi-Spectral Resolution, *Suluh* River Basin

1. Introduction

Land use/land cover (hereafter LULC) change analysis is crucial information for many applications [1, 50, 60]. For example, it can be used to predict future changes, comprehend past LULC changes, and carry out resource management operations [14, 16, 20]. Today, land as a resource becomes the focus of intensified competition from a variety of uses [24] as part of global environmental issues [52, 53, 72]. LULC changes have always there [42] but a rapid LULC change on the current time [11, 52] and as an effect that changes the interaction between the earth systems [53, 60, 64, 75]. The main factor contributing to LULC alterations in Africa was acknowledged to be the conversion of vegetation cover into cultivated land [90].

Investigations into LULC change detection have been conducted in several regions of Ethiopia, with varying results. Thus, the majority of LULC changes in Ethiopia were from natural forests to agricultural land [6, 7, 25, 36, 76, 85, 95] mainly caused by human causes [8, 13, 58, 86, 95]. In contrast, a small number of studies in a separate region of Ethiopia suggested that sustainable land management had improved the vegetation cover [8, 38] due to sustainable land management [3, 82]. The assumption of conversion of the vegetative cover into agricultural land is not always valid as per of various studies. The issue has to be empirically investigated at the level of regional catchments, such as the *Suluh* river basin (hereafter SRB).

Using remote sensing data, there are many techniques enable to make image classification and LULC change detection [15, 27, 48, 49, 62]. The classic (hard) image classification approach as one part of image classification only uses spectral information thereby has less accuracy in classifying multispectral images [30]. Soft image classification has been depicting better accuracy in heterogeneous LULC, continuous nature of geographic features, fragmented lands, and diverse and rugged topography [95]. For instance, object-based [57, 87] classification methods which are based on fuzzy logic are preferable mainly because these methods use spectral, spatial, texture, and contextual, in classifying spectral information [26, 30, 65, 67] and The main use of this soft classifier [2, 4, 24, 49] gives classes' descriptions and giving a membership for each class to express uncertainty [49, 54, 77, 83]. Given that LULC types are nebulous phenomena, numerous academics have argued that fuzzy sets should be used to detect LULC dynamics rather than Boolean sets [16, 20, 46].

The majority of research in Ethiopia was conducted by [5, 11, 13, 23, 29, 51, 66, 80, 84, 94] were followed the pixel-based way of digital image classification and LULC change analysis. Past investigations produced scant evidence due to methodological shortcomings [80]. And, their overall accuracy from recent reports was not excellent as possible [81, 89]. This is because hard image classification faces the problem of mixed pixels, similar spectral information in some features, the continuous nature of the geographic phenomenon, and a lack of exact boundaries among LULC classes [32, 30]. Many researchers have talked about the need to improve classification accuracy for LULC studies throughout the nation [35, 58, 8, 89].

SRB as part of the Ethiopian northern highland and *Tekeze* river basin (Figure 1) is known for its long history of human settlement, very ancient farming system, and war zone which exposed it to deforestation, very severe land degradation, and then the expanding desertification [5]. Additionally, it has heterogonous features, fragmented LULC dominantly substance agriculture, and rugged topography. SRB is subjected to LULC change. Crisp (hard) LULC categorization and analytic technique was employed in a few investigations in the *Tekeze* river basin done by [3, 5, 51, 96]. But, vagueness in the boundaries and the continuous nature of LULC classes are the major problems that affect LULC classification and change analysis. Therefore, this study was conducted; first, to improve the accuracy of LULC classification of land sat image TM (1990), ETM+ (2002), and OLI–TIRS (2018) images using the fuzzy approach in the SRB. Second, to detect LULC change and assesses its driving factors in SRB. In order to achieve sustainable environmental restoration and resource management, we anticipate that the findings of this study will be able to provide policymakers and land managers with useful information.

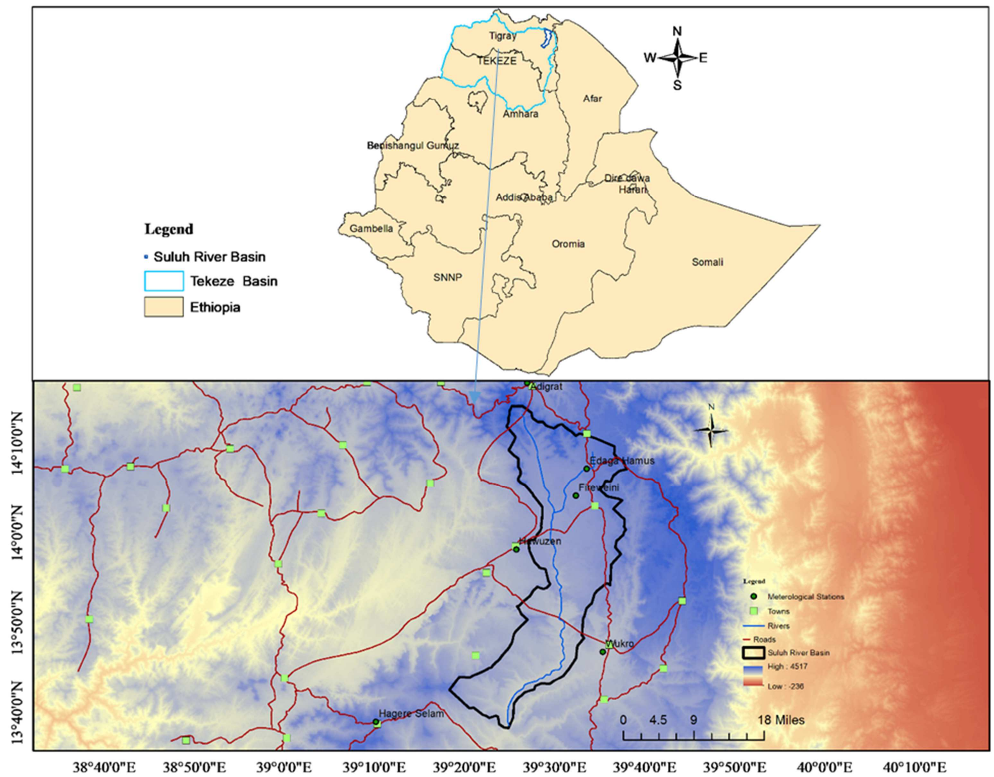

Figure 1. *Location map of Suluh river basin in Tigray, northern Ethiopia.*

2. Materials and Methods

2.1. The Study Area: Suluh River Basin

SRB is found the northeastern part of the Tigray region, northern Ethiopia. SRB's location spans latitudes of 39°24'59.06" and 39°26'22.73", and longitudes of 13°38'18.27" and 14°13'53.29", respectively (Figure 1). SRB covers an area of roughly 930 km^2 and ranges in elevation from 1700 to 3,298 meters above sea level. The study's watershed is located in four districts in Tigray's Eastern and South Eastern zones: *Tsaeda Emba*, *Hawuzen*, *Kiltie Awlealo*, and *Degua Tembien*.

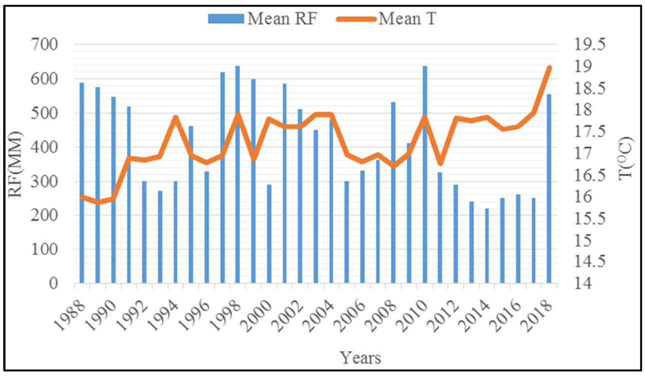

Figure 2. *Total annual rainfall (RF) and Mean Temperature (T) of the Suluh River Basin for the period 1988-2018 (sources station data).*

SRB falls under the category of semi-arid climate. May and June are the warmest months, while December and January are the coldest. From 1988 through 2018, the average annual rainfall total and temperature were 420.4 mm and 17.5°C, respectively (Figure 2). The mono-modal rainfall distribution spans the months of June through early September. The hydrological situation of SRB is dendritic drainage pattern [96]. Trap basalt makes up 2.8% of the basin's geology, followed by granite and shale at 1.8%, metamorphic rock at 28.9%, limestone at 13.9%, and sandstone at 52.7%. *Haplic lixisols* make up 41.4% of the soil in the SRB area, followed by *lithic leptosols* (22.7%), *eutric leptosols* (17.8%), *chromic cambisols* (15.6%), and *vertic cambisols* (2.5%) [96].

According the Ethiopian census of 2007 the population density of SRB was 142 persons/km^2 [18]. The main crops are cultivated in highlands (barley, wheat, maize, *teff*, and pulses) and lowlands (Sorghum). Cultivation is done using the traditional ox-drawn plow [3, 5, 73]. Due to a decrease in vegetation biomass and crop residue, there is a crisis in the supply of feed for livestock (including cattle, sheep, goats, donkeys, and chickens). The vast majority of the regions are intensively farmed, which causes overgrazing and deforestation. The primary methods of land management in SRB include the construction of stone terraces, micro dams, enclosures, and communal woodlots as well as the enforcement of used laws and grazing land limits and reduced burning activities [51, 96, 79].

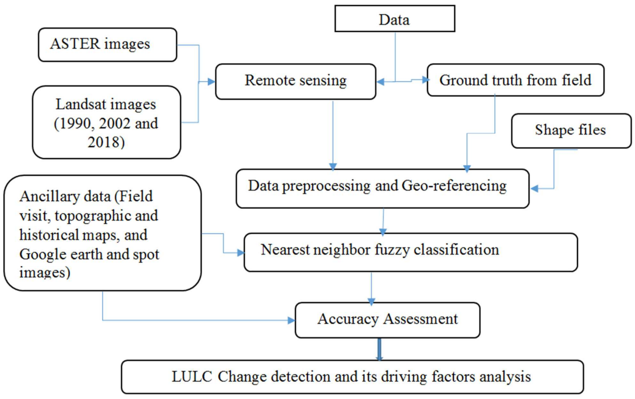

Figure 3. *Flow chart that shows the procedures for LULC change Analysis.*

2.2. Sources of Data

Free satellite photos from the 1990s (Landsat-5 TM), 2002 (Landsat-7 ETM+), and 2018 (Landsat-8 OLI-TIRS) were used for the LULC change study of SRB in accordance with the methods depicted in Figure 3. These files, which included free access to land sat data, were obtained from the National Aeronautics and Space Administration. The 30 meter pixel size of the Landsat-7 ETM$^+$ 2002 and Landsat-8 OLI-TIRS 2018 was resampled to a 30 meter pixel size. Aster imagery-based 30-meter Digital Elevation Model (DEM) was also used. Additionally, auxiliary data were used (Table 1). Three villages from the top, middle, and lower SRB (*Guahgot, Abrha Atsbaha,* and *Adi lal*) were specifically chosen from the primary sources.

Table 1. *The characteristics of land sat satellite data.*

Sensor	Path / row	Acquisition time	Spatial Resolution Resolution	Sensor
Landsat TM	169/50	February/1990	30 m	TM
Landsat ETM+	169/50	February/2002	15 m	ETM$^+$
Landsat OLI-TIRS	169/50	February/2018	15 m	OLI-TIRS
Aster DEM			30 m	
Topo-sheet map			1:50000	
Field data			Nov.2017-Jan 2018	
Road, rivers and town map				
District boundary				
Village boundary				

And, one focus group discussion was prepared and 6 persons participated in each group discussion. The participants were 3 male and 2 female residents as well as one village development agent (Natural resources management expert). A field assessment using Global Positioning System (GPS) was carried out in 2018. Four agricultural and natural resource officers were selected purposely from each district.

2.2.1. Data Processing

To ensure uniformity amongst datasets during analysis, all data were projected using the Universal Transverse Mercator projection system zone 370 N and datum of the World Geodetic System 84 (WGS84). Using ERDAS 2014 software; a thorough pre-processing and processing were performed.

2.2.2. Image Segmentation

Object-based image analysis needs image segmentation [21, 98]. For segmentation, a multi-resolution segmentation was chosen since it maximizes object homogeneity while minimizing average heterogeneity for a specified number of objects [30, 93]. The edited image layer mixing tool of histogram equalizing [21] and six layers mixing were selected. We gave an image layer weight two for the near-infrared band and one for other bands. We used scale parameters (3), shape (0.8), and compactness (0.6) (Table 2).

Table 2. *Parameters used for different images in each segmentation level.*

Sensor	Sc	Sh	Cm Resolution
Landsat TM	3	0.8	0.6
Landsat ETM+	3	0.8	0.6
Landsat OLI-TIRS	3	0.8	0.6

Note: Scale (Sc); Shape (Sh); and Compactness (Cm)

Table 3. *LULC types and their descriptions.*

LU/LC classes	Descriptions
Cultivated land	Areas covered by crops in both irrigation and subsistence farming.
Forest land	Areas covered by forests mainly better canopy
Grazing land	Areas covered by grasses including the closed and free grazing land
Shrubs -bush land	This category contains low woody plants that typically grow vertically and are less than three meters tall with many stems.
Bare land	Vacant spaces with little to no vegetation cover that may also have exposed soil or bedrock.
Built up land	Areas for construction sites and towns
Plantation land	Areas composed of Cactus, *Eucalyptus globules* and *Cupresus spp.*
Water body	Includes lakes (both man-made and natural lakes), rivers, and reserves, among other things.

2.2.3. Fuzzy Classification in eCognition Developer

In this study, we used *eCognition* Developer 9.2 for nearest neighbor fuzzy classification. Fuzzy classification (Eq. 1) was chosen for the analysis of image objects in *eCognition* because translating feature values into fuzzy values, provides adaptable feature [26, 32, 42, 97] and enables the formulation of complex descriptions [54, 77, 98].

$$A=\{(X, \mu A(x)); x \epsilon X\}, \text{ Where } \mu A \rightarrow [0,1] \quad (1)$$

Where A=fuzzy set X=a space of objects X=elements belonging to space X μ – membership function.

The basic steps for nearest neighbor fuzzy-based image classification in *eCognition* include the following steps. The first step is building of knowledge base by defining information classes under the class hierarchy and giving class descriptions. We designed eight LULC classes (cultivated, bar, built up, grazing, plantation, shrub and bush, water body, and forest land) based on Table 3.

The second step is defining the classification condition for each class, nearest neighbor as the classifier is inserted for each class [21]. For the LULC class we used logical operator "and (min)" as well as description of the LULC classes classifier was defined as standard nearest neighbor (here after SNN). And, the "mean value" of the selected feature (6 bands from TM and ETM+ and 7 bands for OLI-TRIS) was used.

The third step is declaring sample objects [21]. Using the nearest neighbor as the classifier is similar to supervised classifications and therefore 20 training areas were selected from each sample of LULC classes. The final step is classification. Before running we applied the edit SNN by selecting object features, layer value, and mean. Next, for all the classes a classifier SNN algorithm was applied [24].

2.2.4. Accuracy Assessment

Assessment of classification accuracy is necessary before it is complete [91] and accuracy evaluation was conducted [19, 61, 68]. ArcGIS 10.5 was used to construct 480 random sample points (60 samples for each LULC class) in order to conduct an accuracy assessment for the classified images. From the related Google Earth images, reference points for the categorized images from 1990, 2002, and 2018 were gathered (i.e. 05 February 1990; 21 February 2002, and 28 February 2018, respectively).

Then, the classified images were compared with the reference images through an error matrix [6, 33, 76, 78]. In this study, overall accuracy (Eq2) and Kappa coefficient (Eq3) were used to assess the accuracy of the classified images. Such methods were applied by [12, 29, 51, 66].

$$\text{OA} = \frac{X}{Y} * 100 \quad (2)$$

Where, OA is overall accuracy, x is number of correct values in diagonals of the matrix, and y is total number of values taken as a reference point.

$$\text{K}=N\sum_{i=1}^{r} xii - \sum_{i=1}^{r}(xi \times x + 1)/\, N2 - \sum_{i=1}^{r} xii - \sum_{i=1}^{r}(xi * x + 1) \quad (3)$$

Where: r = is the number of rows in the matrix

Xii = is the number of observations in rows i and column I (along the major diagonal) Xi+ = the marginal total of row i (right of the matrix)

Xi+1 are the marginal totals of column i (bottom of the matrix) N is the total number of observations. K= kappa coefficient

2.2.5. LULC Change Analysis

The LULC classes were compared in three periods (1990-2002, 2002-2018, and 1990-2018). Change analysis was presented percentages (eq.4) and square kilometers (eq.5) adopted from [36, 57].

$$\text{Percent of change} = \frac{X-Y}{Y} * 100 \quad (4)$$

$$\text{Rate of change} = \frac{X-Y}{Z} \quad (5)$$

Where, X is area of LULC (km^2) in time 2, Y is area of LULC (km^2) in time 1, Z is Time interval between X and Y in years.

LULC conversion matrix between 1990 and 2018 was generated using ArcGIS 10.5 software and compiled in a matrix table, and the values were presented in terms of percentage and square kilometers. The qualitative information collect using were analyzed qualitatively.

3. Results

3.1. Accuracy Assessment

According to Table 4, the classification image's accuracy in 2018 was 90.06% for overall accuracy and 0.886 for the Kappa coefficient. The total accuracy of the classified image in 2002 was 89.8% for overall accuracy, and the Kappa coefficient was 0.883 (Table 4). The classified image's accuracy in 1990 was 87.12% for overall accuracy, and 0.852 for the Kappa coefficient (Table 4). The accuracy of the three classified maps, as reported by the user and producer, ranges from 56% for bare lands in 1990 to 100% for water in 2018 and 55% for cultivated land in 1990 to 100% for water in 2018, respectively.

Table 4. *Summary of error matrixes for the classified images of 1990, 2002 and 2018.*

LULC classes	1990		2002		2018	
	User Accuracy	Producer Accuracy	User Accuracy	Producer Accuracy	User Accuracy	Producer Accuracy
BL	56%	100%	65%	100%	65%	100%
BUL	88%	100%	89%	100%	90%	100%
CL	100%	55%	100%	56%	100%	56%
FL	100%	94%	100%	100%	100%	100%
GL	100%	94%	100%	100%	100%	100%
PL	86%	100%	88%	100%	88%	100%
SBL	78%	100%	79%	100%	80%	100%
WB	94%	100%	100%	100%	100%	100%
Overall Accuracy	87.12121212		89.79592		90.06623	
Kappa Accuracy	0.852591473		0.883327		0.886472	

3.2. LULC Classification and Analysis of SRB

A. LULC classification (1990) and Analysis between 1990 and 2002.

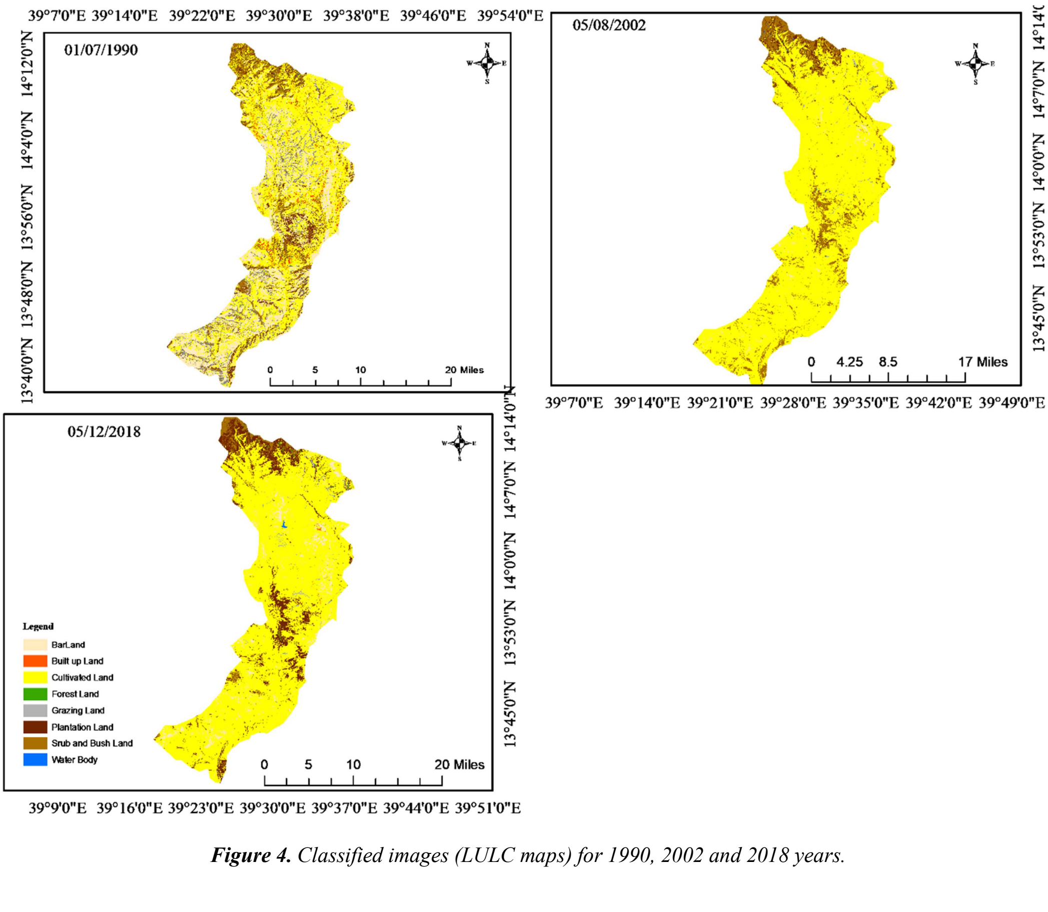

Figure 4. *Classified images (LULC maps) for 1990, 2002 and 2018 years.*

Table 5 and Figure 4 indicated that, in the year of 1990, CL (350.5 km^2) and SBL (219.4 km^2) shares the largest coverage of the LULC type while BUL (12.7 km^2) and WB (7.5 km^2) accounted for the lowest coverage. As Table 4 show that LULC classes like FL, GL, PL, SBL, and WB showed a decrement from 1990 to 2002 by 23.3 km^2, 167.04km^2, 41.64 km^2, 3.34 km^2, 6.4 km^{2}and 35.5 km^2, respectively. Elder priest respondents claimed that in church forests in 1990, there was a better distribution and composition of vegetation. BL, BUL, and CL areas increased between 1990 and 2002 by 8.77 km^2, 229.62 km^2, and 3.73 km^2, respectively. The panelists from the focus group agreed that CL in SRB exhibits high growth. It was also revealed in a planning interview with the district office of agricultural and rural development that the LULCC has been hampered by the population density in the river basin.

B. LULC classification (2002) and Analysis between 2002 and 2018

As it is indicated in Table 5 and Figure 5, in 2002 the largest shares of LULC types were captured by CL accounts at 62.5%, SBL accounts at 23.2% and the smallest coverage was occupied by WB accounts at 0.1% and FL accounts at 0.07%. BUL by13.5 km^2, FL by 9.64 km^2, GL by 76.7 km^2, PL by 62.06 km^2, and WB by 0.39 km^2 showed an increment from 2002 to 2018 (Table 5 and Figure 4). Data gained from the focus group panelist and development agents also confirmed the main causes of natural resources degradation were clearing and selling of wood, free grazing practices and expansions of farmland, people attending their daily life by consuming bulky natural resources, lack of community awareness, due to conflict of interest, lack of construction materials, lack of technical recommendations, and ignorance by respective officials. A reduction of BL by 0.66 km^2, CL km^2 and SBL km^2 was shown from 2002 to 2018. Data gained from the elder farmers also confirmed that the dry-up of *Suluh* River occurred in 2002 years.

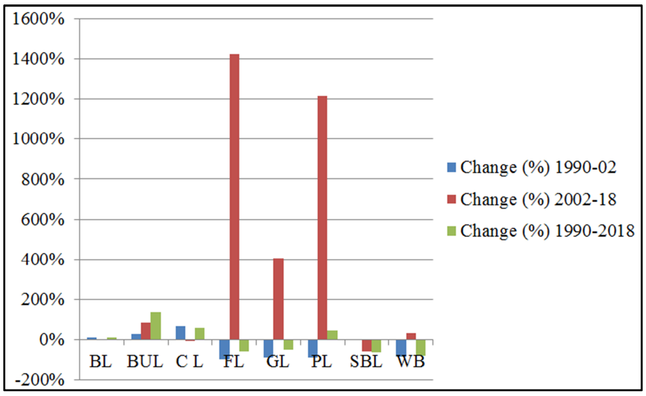

Figure 5. *Trends of LULC changes in SRB.*

C. LULC classification (2018) and Analysis between 1990 and 2018

Table 5 and Figure 4 show that in 2018 the largest LULC classes were occupied by CL and GL while the smallest classes were captured by FL and WB. As shown in Table 4 and Figure 5 BU by 9.8%, BUL by 135.5%, PL by 43.7%, and CL by 7.98% showed an incensement in between 1990-2018. As some farmers interviewed affirmed BL shows an incensement. FGD indicated that proximate and underlined factors lead to LULC change in SRB. FL by 57.67%, GL by 48.6%, SBL by 61.7%, and WB by 79.6% revealed a reduction in between 1990-2018. The data gained from the interviewee showed that most of the formerly WB were drying up. Field observation was made in September 2018 and expansion of PL like Eucalyptus, Cactus *Ruta chalenpensis*, *Rhummus prinoldes,* and coffee were observed.

Table 5. *Classified images for 1990, 2002 and 2018 years and LULC changes between 1990-2002, 2002-2018 and 1990- 2018 in km^2 and percentage.*

Classes	LULC area (km^2)			Change (km^2)			Change (%)		
	1990	2002	2018	1990-02	2002-2018	1990-18	1990-02	2002-2018	1990-18
BL	82.47	91.24	90.56	8.77	-0.66	8.1	10.63	-0.73	9.83
BUL	12.7	16.42	29.9	3.73	13.47	17.2	29.39	82.04	135.53
C L	350.87	580.5	550.81	229.61	-29.68	199.94	65.44	-5.11	56.98
FL	24.4	0.68	10.32	-23.69	9.64	-14.04	-97.22	1425.79	-57.64
GL	185.94	18.9	95.59	-167.04	76.69	-90.35	-89.84	405.84	-48.59
PL	46.74	5.1	67.17	-41.64	62.06	20.42	-89.08	1217.01	43.69
SBL	219.4	216.06	84.13	-3.34	-131.93	-135.27	-1.52	-61.06	-61.66
WB	7.6	1.2	1.54	-6.4	0.39	-6.01	-84.76	33.88	-79.6
Total	930.02		930.02			930.02			

Note: Forest land (FL), cultivated land (CL), shrub-bush land (SBL), built up land (BU), grazing land (GL), bare land (BL), plantation land (PL) and water body (WB)

The change matrix analysis shows that 16% of the land within SRB experienced LULC changes whereas 84% remains unchanged between 1990–2018 years (Table 6). Accordingly Bar land by 9.8%, built upland by 135.5%, plantation land by 43.7%, and cultivated land by 7.98% had shown an increasing trend in between 1990–2018 years. While, forest land by 57.67%, grazing land by 48.6%, shrub and bush land by 61.7%, and water body by 79.6% revealed a reduction trend over the 28 years. As data gained from focus group discussants confirmed that the proximate (increase of farming activity, built-up area and infrastructure expansion, lack of diverse livelihood strategies, unemployment, and drought) and underlined (population pressure and poverty) drivers were leads to LULC change in SRB.

Table 6. *Summary of LULC change matrix in ha from 1990 to 2018.*

From To	BL	BUL	CL	FL	GL	PL	SBL	WB	Total (2018)[b]
BL	8.6	0.1	2.3	0	0	0	0	0	11
BUL	0	0.1	0.1	0	0	0	0	0	0.2
C L	29.6	0.4	735.6	0.1	4.4	27.0	1.4	0.5	799
FL	0	0	0.2	0.3	0.3	0.4	0.1	0	1.2
GL	0	0	1.5	0.1	2.1	0.3	0	0	4
PL	0	0	4.8	0.5	0.3	18.7	2.2	0	26.5
SBL	0	0	21.6	1	0.1	46.8	17.6	0.1	87.2
WB	0	0	0.4	0	0	0.5	0.1	0	1.1
Total (1990)[a]	38.2	0.6	766.5	2	7.1	93.5	21.4	0.6	930.02 Km^2

[a] Row total sums the amount of land for each LULC types of the initial study year (1990); [b] column total sums the amount of land that was converted to each LULC types of the year 2018. The bold diagonal values represent the area of each class that remains unchanged while the off diagonal values represent the change area.

4. Discussion

Eight LULC types were retrieved in SRB using the fuzzy classification method, and the LULC type classification from Landsat images saves resources. We discovered that the kappa coefficient results were extremely accurate. This is due to the method's capacity to depict the data's imprecision by allowing pixels to have a probability of belonging (membership) in more than one class LULC type classification from Landsat image saves resources and eight [31, 45, 63, 70, 83, 87, 88]. Our current study of LULC classification using fuzzy classification were shown better accuracy than prior studies following pixel-based classification method with similar geographical settings and Land sat imageries conducted by [25, 81, 89]. The finding agrees with the studies conducted out of Ethiopia like [2, 15, 45, 70, 77, 83]. Researchers like [41, 42, 59, 63, 77, 83] affirmed that the fuzzy classification approach is applicable for the medium resolution of multispectral land sat images.

BUL, CL, BL, and PL showed an increment trends in between 1990-2018 in *Suluh* river basin at the cost of FL, WB, GL, and SBL. Similar results were confirmed by [5, 9, 10, 12, 22, 24, 27, 28, 34, 37, 39, 47, 51, 85]. Some evidence to the contrary indicated that improved vegetation cover was observed as a result of sustainable land management [11, 38, 69, 71, 82]. In the above studies, there was a difference in the percentage of LULC classes, in the assigning of LULC types, and their way of classification.

Throughout Ethiopia, the factors that are driving LULC change vary from region to region. For instance, human drivers identified by [9, 40, 43, 44, 55, 56]; [17, 18] identified population growth and land degradation; poverty, food insecurity population, slope, livestock, and distances from various infrastructures indicated by [74, 92]; and [36] also identified population pressure, income growth, and declining productivity. In the instance of SRB, the underlined (population pressure and poverty) and proximal (increased farming activity, built-up area and infrastructure expansion, lack of various livelihood strategies, unemployment, and drought) factors were what caused LULC change.

5. Conclusions and Recommendations

LULC classifications using a fuzzy approach in SRB were performed for the years 1990, 2002, and 2018. Despite the medium image resolution, high degree of heterogeneity and fragmented and rugged topography in the study area, general classification accuracy ranges from 88-90% and 0.87-0.89 for overall and kappa coefficient has been achieved, respectively. The results showed that between 1990 and 2018, bar land increased by 9.8%, developed upland increased by 135.5%, plantation land increased by 43.7%, and cultivated land increased by 7.98%. While water bodies by 79.6%, shrub and bush land by 61.7%, pasture land by 48.6%, and forest land by 56.77% showed an upward trend throughout the 28 years, respectively. The LULC changes in SRB were caused by an increase in farming activities, an increase in built-up area and infrastructure, a lack of various livelihood strategies, unemployment and drought, population pressure, and poverty. Therefore, taking into account LULC dynamics data and the corresponding identified causes will aid land use stakeholders in developing better land use planning in SRB.

References

[1] Abebe, S. (2005). Land-Use and Land-Cover change in head stream of Abbay watershed, Blue Nile Basin, Ethiopia. Addis Ababa University.

[2] Al Fugara, A. M., Pradhan, B. and Mohamed, T. A., (2009). Improvement of land-use classification using object-oriented and fuzzy logic approach. *Applied Geomatics*, *1* (4), p. 111.

[3] Alemayehu, F., Taha, N., Nyssen, J., Girma, A., Zenebe, A., Behailu, M., Deckers, S. and Poesen, J., (2009). The impacts of watershed management on land use and land cover dynamics in Eastern Tigray (Ethiopia). *Resources, Conservation and Recycling*, *53* (4), pp. 192-198.

[4] Araya, Y. H. and Hergarten, C., (2008). A comparison of pixel and object-based land cover classification: a case study of the Asmara region, Eritrea. *WIT Transactions on The Built Environment*, *100*, pp. 233-243.

[5] Aredehey, G., Mezgebu, A. and Girma, A., (2018). Land-use land-cover classification analysis of Giba catchment using hyper temporal MODIS NDVI satellite images. *International Journal of Remote Sensing*, *39* (3), pp. 810-821.

[6] Ariti, A. T., van Vliet, J. and Verburg, P. H., (2015). Land-use and land-cover changes in the Central Rift Valley of Ethiopia: Assessment of perception and adaptation of stakeholders. *Applied Geography*, *65*, pp. 28-37.

[7] Belay Taddese (2002). Land-Cover/Land-Use Changes in the Derekolli Catchment. Eastren Africa Social Science Research Review Vol. 18, No. 1.

[8] Bewket, W. (2003). Towards integrated watershed management in highland Ethiopia: the Chemoga watershed case study.

[9] Bewket, W. and Abebe, S., (2013). Land-use and land-cover change and its environmental implications in a tropical highland watershed, Ethiopia. *International journal of environmental studies*, *70* (1), pp. 126-139.

[10] Bewket, W. and Sterk, G., (2005). Dynamics in land cover and its effect on stream flow in the Chemoga watershed, Blue Nile basin, Ethiopia. *Hydrological Processes: An International Journal*, *19* (2), pp. 445-458.

[11] Bewket, W., (2002). Land cover dynamics since the 1950s in Chemoga watershed, Blue Nile basin, Ethiopia. *Mountain research and development*, *22* (3), pp. 263-269.

[12] Birhane, E., Ashfare, H., Fenta, A. A., Hishe, H., Gebremedhin, M. A. and Solomon, N., (2019). Land use land cover changes along topographic gradients in Hugumburda national forest priority area, Northern Ethiopia. *Remote Sensing Applications: Society and Environment*, *13*, pp. 61-68.

[13] Biru, M. K., Minale, A. S. and Debay, A. B., (2015). Multitemporal land use land cover change and dynamics of Blue Nile Basin by using GIS and remote sensing techniques, north-western Ethiopia. *Int. J. Environ. Sci*, *4* (2), pp. 81-88.

[14] Briassoulis, H., (2000). Analysis of Land Use Change: Theoretical and Modeling Approaches. The Web Book of Regional Science.

[15] Buğday, E. and Buğday, S. E., (2019). Modeling and simulating land use/cover change using artificial neural network from remotely sensing data. *Cerne*, *25* (2), pp. 246-254.

[16] Carmel, Y. and Kadmon, R., (1998). Computerized classification of Mediterranean vegetation using panchromatic aerial photographs. *Journal of vegetation Science*, *9* (3), pp. 445-454.

[17] Central Statistics Agency, (1999). Population and Housing Census of Ethiopia, Tigray Region. Addis Ababa, Ethiopia.

[18] Central Statistics Agency, (2015). Population and Housing Census of Ethiopia, Tigray Region. Addis Ababa, Ethiopia.

[19] Congalton, R. G. and Green, K., (2019). *Assessing the accuracy of remotely sensed data: principles and practices*. CRC press.

[20] Das, S., Abraham, A., Chakraborty, U. K. and Konar, A., (2009). Differential evolution using a neighborhood-based mutation operator. *IEEE transactions on evolutionary computation*, *13* (3), pp. 526-553.

[21] Definiens, A. G., (2009). Definiens eCognition developer 8 user guide. *Definens AG, Munchen, Germany*.

[22] Demissie, F., Yeshitila, K., Kindu, M. and Schneider, T., (2017). Land use/Land cover changes and their causes in Libokemkem District of South Gonder, Ethiopia. Remote Sensing Applications: Society and Environment, 8, pp. 224-230.

[23] Denboba, M. A. (2005). Forest Conversion, Soil Degradation, Farmers' Perception Nexus: Implications for Sustainable Land Use in the Southwest of Ethiopia (Vol. 26). Cuvillier Verlag.

[24] Deng, X., (2011). Modeling the dynamics and consequences of land system change (pp. 257-261). Berlin: Springer.

[25] Dessie, G. and Kleman, J., (2007). Pattern and magnitude of deforestation in the South Central Rift Valley Region of Ethiopia. *Mountain research and development*, *27* (2), pp. 162-168.

[26] Doxani, G., Siachalou, S. and Tsakiri-Strati, M., (2008). An object-oriented approach to urban land cover change detection. *Int. Arch. Photogramm. Remote Sens. Spat. Inf. Sci*, *37*, pp. 1655-1660.

[27] Feoli, E., Vuerich, L. G., & Zerihun, W. (2002). Evaluation of environmental degradation in northern Ethiopia using GIS to integrate vegetation, geomorphological, erosion and socio-economic factors. Agriculture, Ecosystems & Environment, 91 (1-3), 313-325.

[28] Fisseha, G., Gebrekidan, H., Kibret, K., Yitaferu, B. and Bedadi, B., (2011). Analysis of land use/land cover changes in the Debre-Mewi watershed at the upper catchment of the Blue Nile Basin, North West Ethiopia. J. Biodivers. Environ. Sci, 1 (6), pp. 184-198.

[29] Fitawok, M. B., Derudder, B., Minale, A. S., Van Passel, S., Adgo, E. and Nyssen, J., (2020). Modeling the Impact of Urbanization on Land-Use Change in Bahir Dar City, Ethiopia: An Integrated Cellular Automata–Markov Chain Approach. *Land*, *9* (4), p. 115.

[30] Flanders, D., Hall-Beyer, M. and Pereverzoff, J., (2003). Preliminary evaluation of eCognition object-based software for cut block delineation and feature extraction. *Canadian Journal of Remote Sensing*, *29* (4), pp. 441-452.

[31] Fleiss, J. L., Levin, B. and Paik, M. C., (2013). *Statistical methods for rates and proportions*. john wiley & sons.

[32] Foody, G. M., (1999). Image classification with a neural network: from completely-crisp to fully-fuzzy situations. *Advances in remote sensing and GIS analysis*, pp. 17-37.

[33] Foody, G. M., (2002). Status of land cover classification accuracy assessment. *Remote sensing of environment*, *80* (1), pp. 185-201.

[34] Garedew, E. (2010). Land-use and land-cover dynamics and rural livelihood perspectives, in the semi-arid areas of Central Rift Valley of Ethiopia (Vol. 2010, No. 7).

[35] Gashaw, T., Tulu, T. and Argaw, M., (2018). Erosion risk assessment for prioritization of conservation measures in Geleda watershed, Blue Nile basin, Ethiopia. *Environmental Systems Research*, *6* (1), p. 1.

[36] Gashaw, T., Tulu, T., Argaw, M., & Worqlul, A. W. (2017). Evaluation and prediction of land use/land cover changes in the Andassa watershed, Blue Nile Basin, Ethiopia. Environmental Systems Research, 6 (1), 17.

[37] Gebrehiwet, K. B. (2004). Land use and land cover changes in the central highlands of Ethiopia: The case of Yerer Mountain and its surroundings. Unpublished MSc. Project Report.

[38] Gebrelibanos, T. and Assen, M., (2015). Land use/land cover dynamics and their driving forces in the Hirmi watershed and its adjacent agroecosystem, highlands of Northern Ethiopia. J Land Use Sci 10 (1): 81–94.

[39] Gessesse, B. and Bewket, W., (2014). Drivers and implications of land use and land cover change in the central highlands of Ethiopia: Evidence from remote sensing and socio-demographic data integration. *Ethiopian Journal of the Social Sciences and Humanities*, *10* (2), pp. 1-23.

[40] Gete Zeleke & Hurni, H. (2001). Implications of land use and land cover dynamics for mountain resource degradation in the Northwestern Ethiopian highlands. Mountain research and development, 21 (2), 184- 191.

[41] Gomarasca, M. A., (2009). Land use/land cover classification systems. In *Basics of Geomatics* (pp. 561-598). Springer, Dordrecht.

[42] Groenemans, R., Van Ranst, E. and Kerre, E., (1997). Fuzzy relational calculus in land evaluation. *Geoderma*, *77* (2-4), pp. 283-298.

[43] Hadgu, K. M. (2008). Temporal and spatial changes in land use patterns and biodiversity in relation to farm productivity at multiple scales in Tigray, Ethiopia. Wageningen Universiteit.

[44] Hamza, I. A. and Iyela, A., (2012). Land use pattern, climate change, and its implication for food security in Ethiopia: A review. *Ethiopian Journal of Environmental Studies and Management*, *5* (1), pp. 26-31.

[45] Han, R., (2014). Land Use and Land Cover Mapping Using Fuzzy Logic. In *Ecosystem Assessment and Fuzzy Systems Management* (pp. 129-146). Springer, Cham.

[46] Hansen, D., Curlis, C. and Simpson, B., (2006). Techniques for discrimination between agriculture and similar land cover types with fuzzy logic and spectral polygon characteristics. In ASPRS 2006 Annual Conference Reno, Nevada.

[47] Hassen, E. E. and Assen, M., (2018). Land use/cover dynamics and its drivers in Gelda catchment, Lake Tana watershed, Ethiopia. *Environmental Systems Research*, *6* (1), p. 4.

[48] Herold, M., Couclelis, H., & Clarke, K. C. (2005). The role of spatial metrics in the analysis and modeling of urban land use change. Computers, Environment and Urban Systems, 29 (4), 369-399.

[49] Hester, D. B., Nelson, S. A. C., Cakir, H. I., Khorram, S. and Cheshire, H., (2010). High-resolution land cover change detection based on fuzzy uncertainty analysis and change reasoning. *International Journal of Remote Sensing*, *31* (2), pp. 455-475.

[50] Hietel, E., Waldhardt, R. and Otte, A., (2004). Analysing land-cover changes in relation to environmental variables in Hesse, Germany. *Landscape ecology*, *19* (5), pp. 473-489.

[51] Hishe, S., Bewket, W., Nyssen, J. and Lyimo, J., (2020). Analysing past land use land cover change and CA-Markov-based future modelling in the Middle Suluh Valley, Northern Ethiopia. *Geocarto International*, *35* (3), pp. 225-255.

[52] Houghton, R. A., (1994). The worldwide extent of land-use change. *BioScience*, *44* (5), pp. 305-313.

[53] Kabat, P., Claussen, M., Dirmeyer, P. A., Gash, J. H., de Guenni, L. B., Meybeck, M., Hutjes, R. W., Pielke Sr, R. A., Vorosmarty, C. J. and Lütkemeier, S. eds., (2004). *Vegetation, water, humans and the climate: A new perspective on an internactive system*. Springer Science & Business Media.

[54] Kalantar, B., Mansor, S. B., Sameen, M. I., Pradhan, B. and Shafri, H. Z., (2017). Drone-based land-cover mapping using a fuzzy unordered rule induction algorithm integrated into object-based image analysis. *International Journal of Remote Sensing*, *38* (8-10), pp. 2535-2556.

[55] Kassa, G. (2003). GIS based analysis of land use and land cover, land degradation and population changes: A study of Boru Metero area of south Wello, Amhara Region MA Thesis, Department of Geography, Addis Ababa University. 110 pp.

[56] Kidanu, S (2004). Using Eucalyptus for soil and water conservation on the highland Vertisols of Ethiopia, PhD Thesis, Wageningen University, The Netherlands.

[57] Kindu, M., Schneider, T., Teketay, D. and Knoke, T., (2013). Land use/land cover change analysis using object-based classification approach in Munessa-Shashemene landscape of the Ethiopian highlands. *Remote Sensing*, *5* (5), pp. 2411-2435.

[58] Kindu, M., Schneider, T., Teketay, D. and Knoke, T., (2015). Drivers of land use/land cover changes in Munessa-Shashemene landscape of the south-central highlands of Ethiopia. *Environmental monitoring and assessment*, *187* (7), p. 452.

[59] Kumar, P., Ravindranath, S. and Raj, K. G., (2018). Object oriented classification and feature extraction for parts of east delhi using hybrid approach. *International Archives of the Photogrammetry, Remote Sensing & Spatial Information Sciences*.

[60] Lambin, E. F., Geist, H. J. and Lepers, E., (2003). Dynamics of land-use and land-cover change in tropical regions. *Annual review of environment and resources*, *28* (1), pp. 205-241.

[61] Lillesand, T. M. and Kiefer, R. W., (2000). Remote Sensing and Image Interpretation, 4th edn (New York: Johy Wiley & Sons).

[62] Lu, D., Mausel, P., Brondizio, E. and Moran, E., (2004). Change detection techniques. International journal of remote sensing, 25 (12), pp. 2365-2401.

[63] Lucieer, A. (2004). Uncertainties in Segmentation and their Visualisation (Doctoral dissertation, Utrecht University and International Institute for Geo-Information Science and Earth Observation (ITC)).

[64] Mahmood, R., Pielke Sr, R. A., Hubbard, K. G., Niyogi, D., Bonan, G., Lawrence, P., McNider, R., McAlpine, C., Etter, A., Gameda, S. and Qian, B., (2010). Impacts of land use/land cover change on climate and future research priorities. Bulletin of the American Meteorological Society, 91 (1), pp. 37-46.

[65] Malik, V., Gautam, A., Sahai, A., Jha, A. and Singh, A., (2013). Satellite Image Classification Using Fuzzy Logic. *International Journal of Recent Technology and Engineering (IJRTE)*, *2* (2), pp. 204-207.

[66] Minale, A. S. and Gelaye, S., (2019). Vegetation vulnerability analysis by using GIS and remote sensing techniques: a case study of Sensawuha Watershed, Ethiopia. *GeoJournal*, pp. 1-14.

[67] Mitri, G. H. and Gitas, I. Z., (2002). The development of an object-oriented classification model for operational burned area mapping on the Mediterranean island of Thasos using LANDSAT TM images. *Forest Fire Research & Wildland Fire Safety*, pp. 1-12.

[68] Mosammam, H. M., Nia, J. T., Khani, H., Teymouri, A. and Kazemi, M., (2016). Monitoring land use change and measuring urban sprawl based on its spatial forms: the case of Qom city. Egypt J Remote Sens Space Sci.

[69] Nega, E., Heluf, G. and Degefe, T., (2012). Analysis of land use/land cover changes in western Ethiopian mixed crop-livestock systems: the case of Senbat watershed. Journal of Biodiversity and Environmental Sciences (JBES), 2 (3), pp. 8-17.

[70] Nilanchal, P., Gadadhar, S. and Singh, A. K., (2013). Image classification for different land use and land covers using fuzzy logic for the improvement of accuracies. *Journal of Agricultural Science (Toronto)*, *5* (3), pp. 278-283.

[71] Nyssen, J., Munro, N., Haile, M., Poesen, J., Descheemaeker, K., Haregeweyn, N., Moeyersons, J., Govers, G. and Deckers, J., (2007). Understanding the environmental changes in Tigray: a photographic record over 30 years. *Tigray Livelihood Papers*, *3*, p. 82.

[72] Paiboonvorachat, C. and Oyana, T. J., (2011). Land-cover changes and potential impacts on soil erosion in the Nan watershed, Thailand. *International journal of remote sensing*, *32* (21), pp. 6587-6609.

[73] Pender, J., Gebremedhin, B., Benin, S. and Ehui, S., (2001). Strategies for sustainable agricultural development in the Ethiopian highlands. American Journal of Agricultural Economics, 83 (5), pp. 1231-1240.

[74] Pender, J., Gebremedhin, B., Benin, S., & Ehui, S. (2001). Strategies for sustainable agricultural development in the Ethiopian highlands. American Journal of Agricultural Economics, 83 (5), 1231-1240.

[75] Prasad, P. R. C., Rajan, K. S., Dutt, C. B. S. and Roy, P. S., (2010). A conceptual framework to analyse the land-use/land-cover changes and its impact on phytodiversity: a case study of North Andaman Islands, India. Biodiversity and conservation, 19 (11), pp. 3073-3087.

[76] Rientjes, T. H. M., Haile, A. T., Kebede, E., Mannaerts, C. M. M., Habib, E. and Steenhuis, T. S., (2011). Changes in land cover, rainfall and stream flow in Upper Gilgel Abbay catchment, Blue Nile basin--Ethiopia. *Hydrology & Earth System Sciences*, *15* (6).

[77] Salman, A. A., Ali, A. E. and Mattar, H. E., (2008). Mapping land-use/land-cover of Khartoum using fuzzy classification. *Emirates Journal for Engineering Research, 13 (2), 27, 43.*

[78] Schulz, J. J., Cayuela, L., Echeverria, C., Salas, J. and Benayas, J. M. R., (2010). Monitoring land cover change of the dryland forest landscape of Central Chile (1975–2008). *Applied Geography*, *30* (3), pp. 436-447.

[79] Sembroni, A., Molin, P., Dramis, F. and Abebe, B., (2017). Geology of the Tekeze river basin (northern Ethiopia). *Journal of Maps*, *13* (2), pp. 621-631.

[80] Sewnet, A. and Abebe, G., (2018). Land use and land cover change and implication to watershed degradation by using GIS and remote sensing in the Koga watershed, North Western Ethiopia. *Earth Science Informatics*, *11* (1), pp. 99-108.

[81] Shiferaw, A. and Singh, K. L., (2011). Evaluating the land use and land cover dynamics in Borena Woreda South Wollo Highlands, Ethiopia. *Ethiopian Journal of Business and Economics (The)*, *2* (1).

[82] Tadele, M., Birhane, E., Kidu, G., G-Wahid, H. and Rannestad, M. M., (2020). Contribution of parkland agroforestry in meeting fuel wood demand in the dry lands of tigray, ethiopia. Journal of Sustainable Forestry, pp. 1-13.

[83] Taufik, A. and Ahmad, S. S. S., (2016). Land cover classification of Landsat 8 satellite data based on Fuzzy Logic approach. In *IOP Conf. Ser. Earth Environ. Sci* (Vol. 37, p. 12062).

[84] Teferi, E., Uhlenbrook, S., Bewket, W., Wenninger, J. and Simane, B., (2010). The use of remote sensing to quantify wetland loss in the Choke Mountain range, Upper Blue Nile basin, Ethiopia. *Hydrology and Earth System Sciences*, *14* (12), pp. 2415-2428.

[85] Tekle, K. and Hedlund, L. (2000). Land Cover Changes between 1958 and 1986 in Kalu District, Southern Wello, Ethiopia. Mountain Research and Development, 20 (1): 42 - 51.

[86] Tekle, K. and Hedlund, L., (2004). Land cover changes between 1958 and 1986 in Kalu District, southern Wello, Ethiopia. Mountain research and development, 20 (1), pp. 42-51.

[87] Tewolde, M. G. and Cabral, P., (2011). Urban sprawl analysis and modeling in Asmara, Eritrea. *Remote Sensing*, *3* (10), pp. 2148-2165.

[88] Verburg, P. H., Soepboer, W., Veldkamp, A., Limpiada, R., Espaldon, V., & Mastura, S. S. (2002). Modeling the spatial dynamics of regional land use: the CLUE-S model. Environmental management, 30 (3), 391-405.

[89] Wondie, M., Schneider, W., Melesse, A. M. and Teketay, D., (2011). Spatial and temporal land cover changes in the Simen Mountains National Park, a world heritage site in Northwestern Ethiopia. *Remote Sensing*, *3* (4), pp. 752-766.

[90] Wood, E. C., Tappan, G. G. and Hadj, A., (2004). Understanding the drivers of agricultural land use change in south-central Senegal. Journal of Arid Environments, 59 (3), pp. 565-582.

[91] Xiuqina, W., Yunlong, C. and Tao, Z., (2011). Effects of land use/land cover changes on rocky desertification-a case study of a small Karst catchment in Southwestern China. Energy Procedia, 5, pp. 1-5.

[92] Yalew, S. G., Mul, M. L., van Griensven, A., Teferi, E., Priess, J., Schweitzer, C., & van Der Zaag, P. (2016). Land-Use Change Modelling in the Upper Blue Nile Basin. Environments, 3 (3), 21.

[93] Yan, G., Mas, J. F., Maathuis, B. H. P., Xiangmin, Z. and Van Dijk, P. M., (2006). Comparison of pixel-based and object-oriented image classification approaches—a case study in a coal fire area, Wuda, Inner Mongolia, China. *International Journal of Remote Sensing*, *27* (18), pp. 4039-4055.

[94] Yesuph, A. Y. and Dagnew, A. B., (2019). Land use/cover spatiotemporal dynamics, driving forces and implications at the Beshillo catchment of the Blue Nile Basin, North Eastern Highlands of Ethiopia. *Environmental Systems Research*, *8* (1), p. 21.

[95] Zeleke, G. and Hurni, H., (2001). Implications of land use and land cover dynamics for mountain resource degradation in the Northwestern Ethiopian highlands. Mountain research and development, 21 (2), pp. 184-191.

[96] Zenebe, A., Vanmaercke, M., Guyassa, E., Verstraeten, G., Poesen, J. and Nyssen, J., (2019). The Giba, Tanqwa and Tsaliet Rivers in the Headwaters of the Tekezze Basin. In *Geo-trekking in Ethiopia's Tropical Mountains* (pp. 215-230). Springer, Cham.

[97] Zhang, J. and Foody, G. M., (1998). A fuzzy classification of sub-urban land cover from remotely sensed imagery. *International journal of remote sensing*, *19* (14), pp. 2721-2738.

[98] Zhou, W., Troy, A. and Grove, M., (2008). Object-based land cover classification and change analysis in the Baltimore metropolitan area using multitemporal high resolution remote sensing data. Sensors, 8 (3), pp. 1613-1636.